Stanniocalcin-1 suppresses TGF-β-induced mitochondrial dysfunction and cellular fibrosis in human renal proximal tubular cells

EUN MI YANG[1], JUNG SUN PARK[2], SOO YEON JOO[2], EUN HUI BAE[2], SEONG KWON MA[2] and SOO WAN KIM[2]

Departments of [1]Pediatrics and [2]Internal Medicine, Chonnam National University Medical School, Gwangju 61469, Republic of Korea

Received December 31, 2021; Accepted April 29, 2022

DOI: 10.3892/ijmm.2022.5163

Abstract. Stanniocalcin-1 (STC1), a multifunctional glycoprotein with antioxidant and anti-inflammatory properties, serves an important role in kidney protection. STC1 is one of the few hormones targeted to the mitochondria to regulate mitochondrial quality control by suppressing oxidative stress and mitochondrial damage. However, the mechanisms underlying the effect of STC1 remain unclear. The present study aimed to investigate the protective role of recombinant STC1 (rSTC1) in renal fibrosis and to identify the mechanisms underlying cellular fibrosis in HK2 human renal proximal tubular cells. Semi-quantitative PCR, western blot analysis and confocal microscopy were used to detect the mRNA levels, protein levels and mitochondrial membrane potential (MMP). Mitochondrial superoxide production was evaluated using MitoSox staining. rSTC1 attenuated TGF-β-induced downregulation of AMP-activated protein kinase and uncoupling protein 2 (UCP2). Treatment of HK2 cells with TGF-β reduced the MMP and increased the production of reactive oxygen species (ROS). In addition, TGF-β treatment upregulated fibrotic markers, such as α-SMA and fibronectin, in HK2 cells. Treatment with rSTC1 and TGF-β suppressed mitochondrial ROS production by recovering the MMP and reversed the upregulation of fibrotic markers in HK2 cells. The effects of rSTC1 were reversed when UCP2 expression was silenced. The present study revealed a novel role of STC1 in preventing TGF-β induced cellular fibrosis in HK2 cells.

Correspondence to: Dr Soo Wan Kim, Department of Internal Medicine, Chonnam National University Medical School, 42 Jebongro, Dong-gu, Gwangju 61469, Republic of Korea
E-mail: skimw@chonnam.ac.kr

Key words: stanniocalcin-1, mitochondria, fibrosis, reactive oxygen species, antioxidant

Introduction

Chronic kidney disease (CKD) results from a variety of disorders that affect the structure and function of the kidneys and represents a rising global health concern due to its increasing prevalence (8-16%) (1). There is no cure for CKD and the available therapies only aim to slow disease progression. The progressive nature of CKD, as well as its associated cardiovascular morbidity and mortality and eventual end-stage renal disease place a substantial burden on global healthcare resources (2,3). An improved understanding of the nature of CKD is required for the development of novel therapeutic strategies. All types of progressive CKD inevitably induce renal fibrosis (4). The induction of renal fibrosis due to mitochondrial dysfunction has received considerable research attention since the early 2000s (5). The kidney is an organ with high energy demand. Mitochondria provide the energy required to maintain kidney function via a number of signaling pathways, such as the mechanistic target of rapamycin and AMP-activated protein kinase (AMPK) signaling pathways (6). Aberrations in energy metabolism can lead to cellular dysfunction and death. Mitochondria not only produce cellular energy but also modulate several cellular processes, including proliferation and intracellular calcium homeostasis (7). Mitochondrial dysfunction induces apoptosis and the generation of reactive oxygen species (ROS), both of which contribute to the development and progression of various kidney diseases, including acute kidney injury, diabetic nephropathy and CKD (6,8-11). Reversing mitochondrial dysfunction has the potential to halt disease progression, emphasizing the need for mitochondria-targeting agents that can restore mitochondrial and renal function (7).

Stanniocalcin-1 (STC1) was originally identified as a calcium/phosphate-regulating hormone in bony fishes and is released from the corpuscles of Stannius (organs associated with kidneys) (12). In mammals, STC1 is expressed in various tissues (12) and is considered to function in an autocrine and/or paracrine manner (13); however, the localization of STC1 to mitochondria suggests a possible intracellular role (14). STC1 is one of the few hormones that target the mitochondrion (15) and demonstrates antioxidant effects via activation of mitochondrial antioxidant pathways (16-18). STC1 regulates AMPK activity in the kidneys (19) and suppresses ROS generation via

the induction of the mitochondrial uncoupling protein (UCP) in macrophages (16,17). The aims of the present study were to ascertain whether STC1 reduces TGF-β-induced cellular fibrosis in the kidney tubular epithelial cells by reducing mitochondrial oxidative stress and mitochondrial damage and to explore the associated molecular mechanisms.

Materials and methods

Reagents and antibodies. Recombinant human TGF-β was purchased from PeproTech EC Ltd. (cat. no. 100-21) and recombinant STC1 (rSTC1; MBS1265316) was purchased from MyBioSource, Inc. AMPK inhibitor (ab120843) was purchased from Abcam. UCP2-targeted small interfering RNA (siRNA) (siUCP2) was purchased from GE Healthcare Dharmacon, Inc. (cat. no. L-005114-00-0020). Anti-fibronectin (610077) and anti-UCP2 antibodies (sc-390189) were obtained from BD Biosciences and Santa Cruz Biotechnology, Inc. Antibodies against α-smooth muscle actin (α-SMA; a2547) and β-actin (a3854) were obtained from MilliporeSigma. Anti-AMPK (cat. no. 2793) and anti-phosphorylated AMPK (recognizing phosphorylated Thr172; cat. no. 2535) antibodies were purchased from Cell Signaling Technology, Inc.

Cell culture and TGF-β treatment. Human renal proximal tubular epithelial cells (HK2, American Type Culture Collection) were cultured in complete DMEM-F12 (Welgene, Inc.) supplemented with 10% FBS (Thermo Fisher Scientific, Inc.), 50 U/ml penicillin and 50 μg/ml streptomycin (MilliporeSigma) at 37˚C in a humidified 5% CO_2 atmosphere. Cells were passaged every 3-4 days and starved in serum-free medium for 24 h before experiments. TGF-β is the central mediator that drives fibrosis in most, if not all, forms of CKD (20). To investigate the role of STC1 in the AMPK pathway, the expression levels of AMPK and UCP2 were analyzed at different time points (0 min, 15 min, 30 min, 1 h, 3 h and 6 h) following TGF-β and rSTC1 treatment. To identify whether STC1 suppressed TGF-β-induced mitochondrial dysfunction and fibrosis, HK2 cells were pre-incubated at 37˚C with 200 ng/ml STC1 for 1 h and then incubated at 37˚C with fresh medium containing 10 ng/ml TGF-β for 16 h. To determine whether the effect of STC1 was mediated by AMPK activation, pharmacological inhibition of AMPK by compound C (Calbiochem; Merck KGaA) was performed. Compound C (5 μM/ml) was added to HK2 cells at 37˚C for 1 h and then cells were pre-incubated at 37˚C with 200 ng/ml STC1 for 1 h and subsequently incubated at 37˚C with fresh medium containing 10 ng/ml TGF-β for 16 h.

siRNA transfection. To explore the molecular mechanisms underlying the effects of STC1, RNA interference was performed using a pool of UCP2-specific siRNAs from On-TargetPlus Human SmartPools containing 4 distinct siRNA species (cat. no. L-005114-00-0020). The negative control siRNA was purchased from Santa Cruz Biotechnology, Inc. (cat. no. sc 37007). siRNA sequences of UCP2 are described in Table SI. Cells were transfected with the indicated concentration of siRNA (40 nM) using DharmaFECT 1 transfection reagent according to the manufacturer's protocol. For knockdown of UCP2, siRNA and control siRNA were transfected into HK-2 cells at 60% confluence at 37˚C in a 5% CO_2 incubator for 24 h using DharmaFECT 1 transfection reagent (T-2001-02; GE Healthcare Dharmacon, Inc.) at a final concentration of 40 nM. After transfection, cells were incubated in serum-free medium for 1 day in a 37˚C incubator under a humidified 5% CO_2 atmosphere, pretreated at 37˚C with 200 ng/ml STC1 for 1 h and stimulated at 37˚C with 10 ng/ml TGF-β for 16 h. Confirmation of Successful transfection of siRNA in HK-2 cells was determined using semi-quantitative PCR and western blotting as described subsequently in this section (Fig. S1).

Semi-quantitative PCR. Total RNA was extracted from HK-2 cells using TRIzol reagent (Invitrogen; Thermo Fisher Scientific, Inc.). First-standard complementary DNA synthesis was performed using a SuperScript™ First-Strand Synthesis System kit (cat. no. 11904-018; Invitrogen; Thermo Fisher Scientific, Inc.). Total RNA (1 μg) was used for first-strand complementary DNA synthesis and First-Strand Synthesis reaction (10 mM dNTP mix, 50 ng/μl random hexamers, 10 X RT buffer, 25 mM $MgCl_2$, 0.1 M DTT, 40 U/μl RNaseOUT™, SuperScript™ II RT, DEPC-treated water) was used. After incubation at 42˚C for 50 min, the reaction was completed by incubation at 70˚C for 15 min to prepare complementary DNA. The specific steps followed the SuperScript™ First-Strand Synthesis System kit manufacturer's protocol. UCP2 expression was normalized to that of β-actin. The specific primers sequences were as follows: UCP2 forward, 5'-TCTACAATG GGCTGGTTGC-3' and reverse, 5'-TGTATCTCGTCTTGA CCAC-3' (494 bp); and β-actin forward, 5'-GCTCTTTTCCAG CCTTCCTT-3' and reverse, 5'-AGTACTTGCGCTCAGGAG GA-3' (234 bp). After an initial denaturation step of 5 min at 94˚C, semi-quantitative PCR amplification was carried out as follows: 95˚C for 30 sec, 56˚C for 30 sec and 72˚C for 30 sec for 35 cycle, followed by one cycle at 72˚C for 5 min. A 1% agarose gel was used for DNA loading, and SYBR DNA gel stain (cat. no. S33102; Invitrogen; Thermo Fisher Scientific, Inc.) was used for visualization. The relative intensities of DNA were measured by densitometry using Scion Image for Windows (version Alpha 4.0.3.2; Scion Corporation).

Western blotting. The cells were harvested, washed twice with ice-cold PBS, resuspended in lysis buffer and sonicated briefly. Protein extraction buffer consisted of 50 mM Tris-HCl (pH 7.2), 5 mM EDTA, 150 mM NaCl, 1% Nonidet P-40, 0.1% SDS, protease inhibitor cocktail (P3100-001; GenDEPOT, LLC) and phosphatase inhibitor cocktail (P3200-001; GenDEPOT, LLC). After centrifugation at 4˚C at 13,500 x g for 5 min, supernatants containing the protein extracts were collected and the protein concentrations were measured using a Pierce® BCA Protein Assay kit (Pierce; Thermo Fisher Scientific, Inc.). Proteins were separated on 10 and 12% sodium dodecyl sulfate polyacrylamide gels, and transferred onto nitrocellulose membranes. The protein concentration loaded per lane was 30 μg, and the blot was blocked at room temperature for 1 h with 5% skim milk in PBS containing 0.1% Tween-20. Then, the blots were incubated overnight with the primary antibody (1:2,000) at 4˚C, washed four times at 10 min intervals in 1X TBS with 0.1% Tween-20 (TBST) at room temperature, and incubated with appropriate anti-rabbit IgG, HRP-linked

secondary antibody (1:2,500; 7074S; Cell Signaling Technology, Inc.) and anti-mouse IgG, HRP-linked secondary antibody (1:2,500; 7076S; Cell Signaling Technology, Inc.) at room temperature for 2 h. After that, the blots were washed four times in 1X TBST at 10 min intervals. Specific protein bands were visualized using an enhanced chemiluminescence system (cat. no. WBKLS0500; MilliporeSigma). The relative intensities of immunoblot signals were measured by densitometry using Scion Image for Windows (version Alpha 4.0.3.2; Scion Corporation) and were expressed as fold-change values relative to the intensities of the controls.

Quantification of mitochondrial membrane potential (MMP). MMP was assessed using a Leica TCS SP8 confocal laser-scanning microscope (Leica Microsystems GmbH) with 5,5',6,6'-tetrachloro-1,1',3,3'-tetraethylbenzimidazolecarbocyanide iodine (10009172; JC-1 MMP Assay kit; Cayman Chemical Company). HK2 cells were seeded at a density of $3x10^5$ cells/well in a 35-mm confocal special dish, followed by a 24-h incubation at 37˚C. Cells were pretreated with or without 10 ng/ml TGF-β and 200 ng/ml rSTC1 and, then incubated for 16 h at 37˚C with 5% CO_2. Cell nuclei were stained with 2 μg/ml Hoechst 33258 for 20 min in a CO_2 incubator at 37˚C. Slides were analyzed with a confocal laser scanning microscope (Leica TCS SP8; Leica Microsystems GmbH) and LAS X software (version 4.0.2; Leica Microsystems GmbH) was used. Fluorescence was read at an excitation wavelength of 488 nm (green) or 530 nm (red) and an emission wavelength of 530 nm (green) or 590 nm (red). JC-1 emits green fluorescence in the cytoplasm and exhibits membrane potential-dependent accumulation in mitochondria, resulting in a shift in the emission wavelength from green to red. A reduction in MMP is indicated by a decrease in the red/green fluorescence intensity ratio (21).

Mitochondrial ROS production. Mitochondrial ROS levels were measured using MitoSOX, which selectively reacts with superoxide in the mitochondria. HK2 cells were seeded at a density of $3x10^5$ cells/well on a cover-glass bottom dish and grown to 60% confluence. After incubation at 37˚C for 24 h, cells were pretreated with or without 10 ng/ml TGF-β and 200 ng/ml rSTC1 and incubated for 16 h at 37˚C with 5% CO_2. The cells were then incubated with 5 μM MitoSOX for 15 min at 37˚C and fixed with 4% paraformaldehyde for 10 min at 37˚C. After fixation, cells were permeabilized with 0.1% Triton X-100 for 10 min and blocked in 1X PBS containing 5% BSA (cat. no. ALB001; BioShop Canada Inc.) for 2 h at room temperature. The cells were then washed twice with phosphate-buffered saline and incubated with 1 μg/ml DAPI solution at 4˚C for 15 min. Images were immediately acquired by confocal microscopy on a laser-scanning microscope (LSM 510; Carl Zeiss AG) and analyzed using ImageJ (version 1.53; National Institutes of Health).

Statistical analysis. All experiments were independently replicated at least three times. Data are presented as the mean ± standard error of the mean. Multiple comparisons among the groups were performed by one-way analysis of variance followed by Tukey's post hoc tests. All statistical analyses were performed using SPSS version 24.0 (IBM Corp.). P<0.05 was considered to indicate a statistically significant difference.

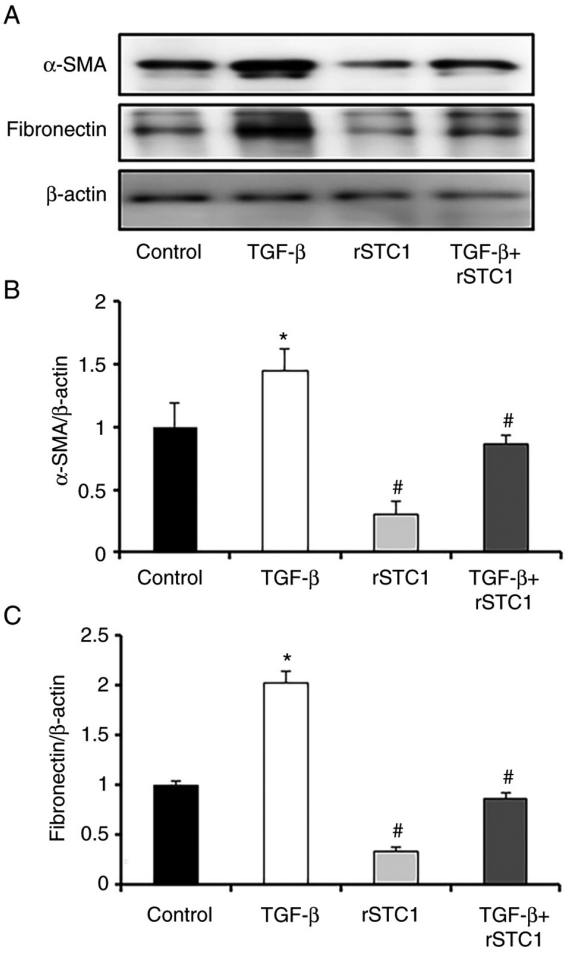

Figure 1. Expression of profibrotic markers in TGF-β-induced fibrosis in HK2 cells. (A) Protein expression levels of α-SMA and fibronectin were analyzed. (B) Relative α-SMA protein expression levels normalized against β-actin levels. (C) Relative fibronectin protein expression levels normalized against β-actin levels. Results are presented as the mean ± SEM of three individual experiments. *P<0.05 compared with the control; #P<0.05 compared with the TGF-β-only-treated cells. α-SMA, α-smooth muscle actin; rSTC1, recombinant stanniocalcin-1.

Results

rSTC1 inhibits TGF-β-induced fibrosis in HK2 cells. To determine whether rSTC1 inhibited fibrotic progression in HK-2 cells, the effects of rSTC1 on TGF-β-induced α-SMA and fibronectin expression in HK2 cells were assessed. The protein expression levels of α-SMA and fibronectin were higher in the TGF-β-only-treated group than in the control group (Fig. 1). Treatment with rSTC1 alone did not affect the protein levels of α-SMA and fibronectin (Fig. 1); however, treatment with rSTC1 and TGF-β together restored the levels of α-SMA and fibronectin to those in the control group.

rSTC1 attenuates the TGF-β-induced suppression of AMPK-UCP2-dependent signaling. Cultured HK2 cells were treated with rSTC1 for different durations (0 min, 15 min, 30 min, 1 h, 3 h and 6 h). While TGF-β repressed AMPK activity for 6 h (Fig. 2A), rSTC1 significantly upregulated

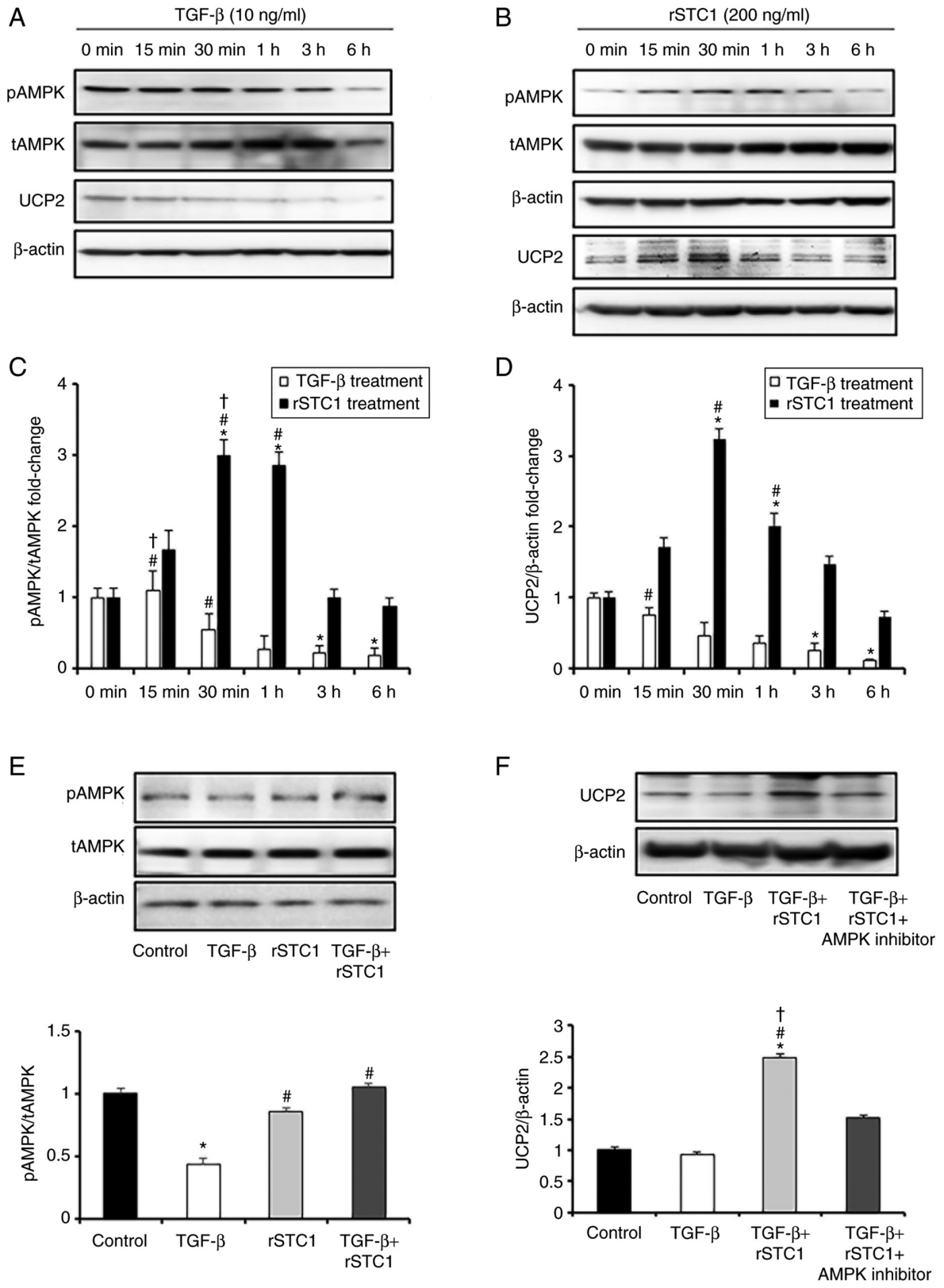

Figure 2. Effects of rSTC1 on the AMPK/UCP2 signaling pathway in HK2 cells. (A) Protein expression levels of AMPK and UCP2 in TGF-β-only-treated HK2 cells at the indicated time points, as determined using western blotting. (B) Protein expresison level of AMPK and UCP2 in rSTC1-treated HK2 cells at the indicated time points, as determined using western blotting. (C) Bar graph of ratio of pAMPK/tAMPK in TGF-β-only-treated and rSTC1-treated HK2 cells at the indicated time points. (D) Bar graph of protein expression levels of UCP2 in TGF-β-only-treated and rSTC1-treated HK2 cells at the indicated time points. *P<0.05 compared with 0 min. #P<0.05 compared with 6 h. †P<0.05 compared with 3 h. (E) Ratio of pAMPK/tAMPK in response to TGF-β and rSTC1 treatment after 6 h, as determined using western blotting. Relative protein expression levels are shown, with the densitometric values normalized to the respective β-actin values. *P<0.05 compared with the control; #P<0.05 compared with TGF-β-only-treated cells. (F) Protein expression levels of UCP2 in response to TGF-β, rSTC1, and AMPK inhibitor treatment after 6 h, as determined using western blotting. Relative protein expression levels are shown, with the densitometric values normalized to the respective β-actin values. *P<0.05 compared with the control; #P<0.05 compared with TGF-β-only-treated cells; †P<0.05 compared with TGF-β, rSTC1 and AMPK inhibitor-treated cells. AMPK, AMP-activated protein kinase; rSTC1, recombinant stanniocalcin-1; pAMPK, phosphorylated AMPK; tAMPK, total AMPK; UCP2, uncoupling protein 2.

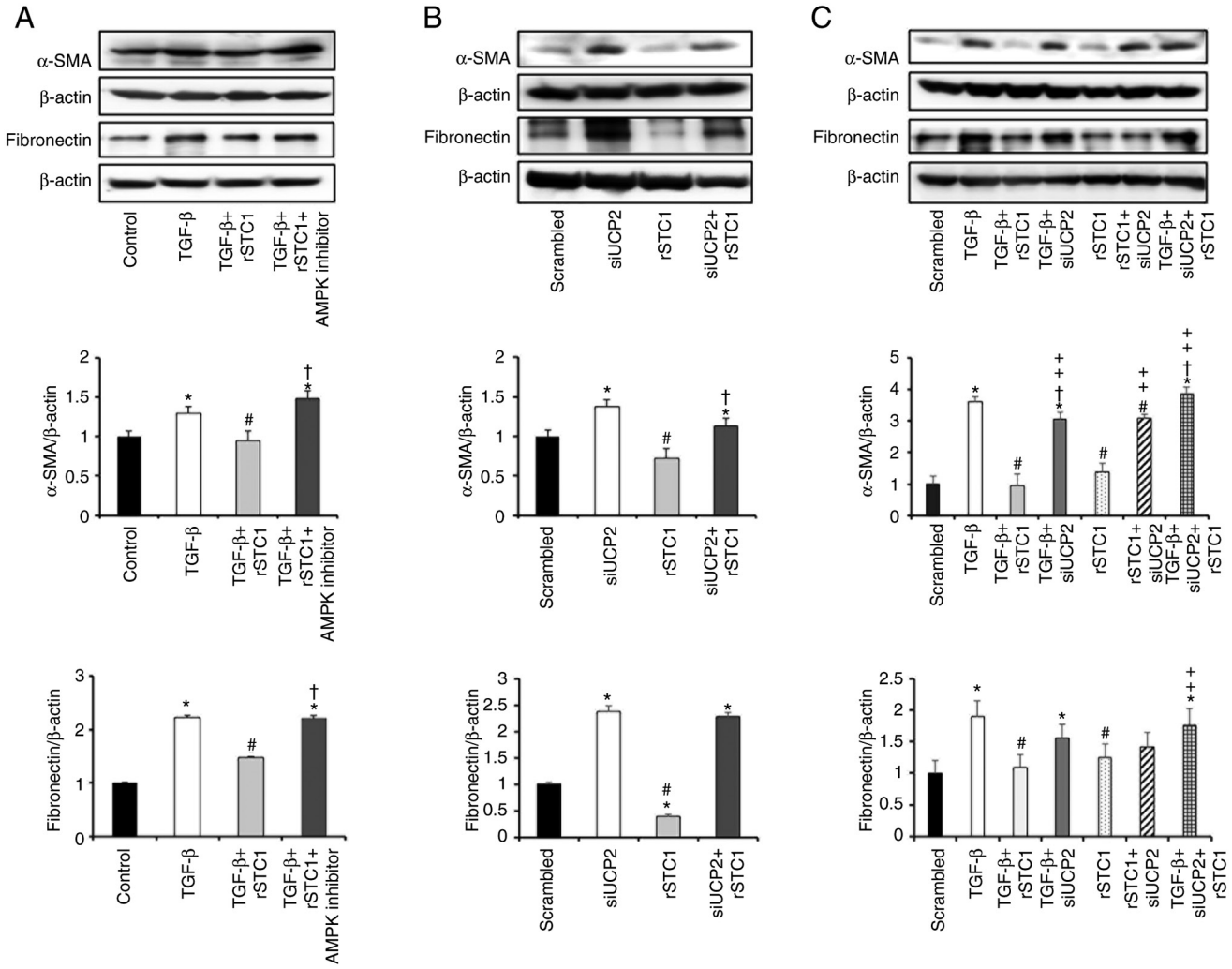

Figure 3. Effect of rSTC1 on the fibrotic signaling pathway in HK2 cells. (A) HK-2 cells were exposed to 10 ng/ml TGF-β for 16 h with or without pre-treatment with 200 ng/ml rSTC1 or 5 μM AMPK inhibitor for 1 h. Western blot analysis of the protein expression levels of α-SMA and fibronectin after AMPK inhibitor treatment. *P<0.05 compared with the control; #P<0.05 compared with TGF-β-only-treated cells; †P<0.05 compared with TGF-β and rSTC1-treated cells. (B) Expression levels of α-SMA and fibronectin, profibrotic marker proteins, after 48 h of transient transfection with siUCP2 in HK-2 cells. The blots indicated an increase in profibrotic marker expression after UCP2 inhibition. *P<0.05 compared with scrambled; #P<0.05 compared with siUCP2-transfected cells; †P<0.05 compared with rSTC1. (C) Cells were pre-treated with rSTC1 for 1 h with or without transient transfection with siUCP2 for 48 h followed by exposure to TGF-β (10 ng/ml for 16 h). The blots indicated the protein expression levels of α-SMA and fibronectin. Relative protein expression levels are shown, with the densitometric values normalized to the respective β-actin values. Each column represents the mean ± SEM. *P<0.05 compared with the control; #P<0.05 compared with TGF-β-only-treated cells; †P<0.05 compared with the TGF-β and rSTC1-treated cells; ‡P<0.05 compared with the rSTC1-treated cells. α-SMA, α-smooth muscle actin; AMPK, AMP-activated protein kinase; siUCP2, UCP2-targeted small interfering RNA; rSTC1, recombinant stanniocalcin-1; UCP2, uncoupling protein 2.

AMPK activity by nearly 3-fold after treatment for 30 min to 1 h (Fig. 2B). UCP2 expression was also decreased after TGF-β treatment and upregulated after rSTC1 treatment at certain time points (30 min to 1 h). Similar to AMPK activity, the peak level of UCP2 was reached 30 min after rSTC1 treatment (Fig. 2C and D). Treatment with rSTC1 and TGF-β together prevented the TGF-β-induced reduction in AMPK activity in HK2 cells (Fig. 2E). AMPK has been reported to upregulate UCP2 in the kidneys (19). To determine whether the activation of AMPK mediated the upregulation of UCP2, HK2 cells were treated with the AMPK inhibitor, STC1, and TGF-β. Treatment with the AMPK inhibitor diminished the upregulation of UCP2 compared with that observed after treatment with rSTC1 and TGF-β in combination (Fig. 2F). These results indicate that rSTC1 induces AMPK activation and the AMPK-mediated induction of UCP2 expression.

UCP2 inhibition decreases the effects of STC1 on TGF-β-induced fibrosis in HK2 cells. STC1 regulates renal AMPK-UCP2 activity (19), and AMPK activation may inhibit renal fibrosis (22). To determine whether rSTC1 inhibits fibrotic progression via an AMPK-UCP2-dependent pathway, cells were treated with an AMPK inhibitor. The STC1-mediated attenuation of TGF-β-induced upregulation of α-SMA and fibronectin was reversed by AMPK inhibition (Fig. 3A). To reveal the function of UCP2 in suppressing fibrosis, UCP2 was knocked down using a siRNA (siUCP2). HK2 cells were transfected with either scrambled siRNA or siUCP2. siUCP2 transfection resulted in the upregulation of α-SMA and fibronectin compared with scrambled-siRNA-transfected cells. Treatment of siUCP2-transfected cells with rSTC1 increased the expression levels of α-SMA and fibronectin compared with those in cells treated with rSTC1 alone (Fig. 3B). The treatment

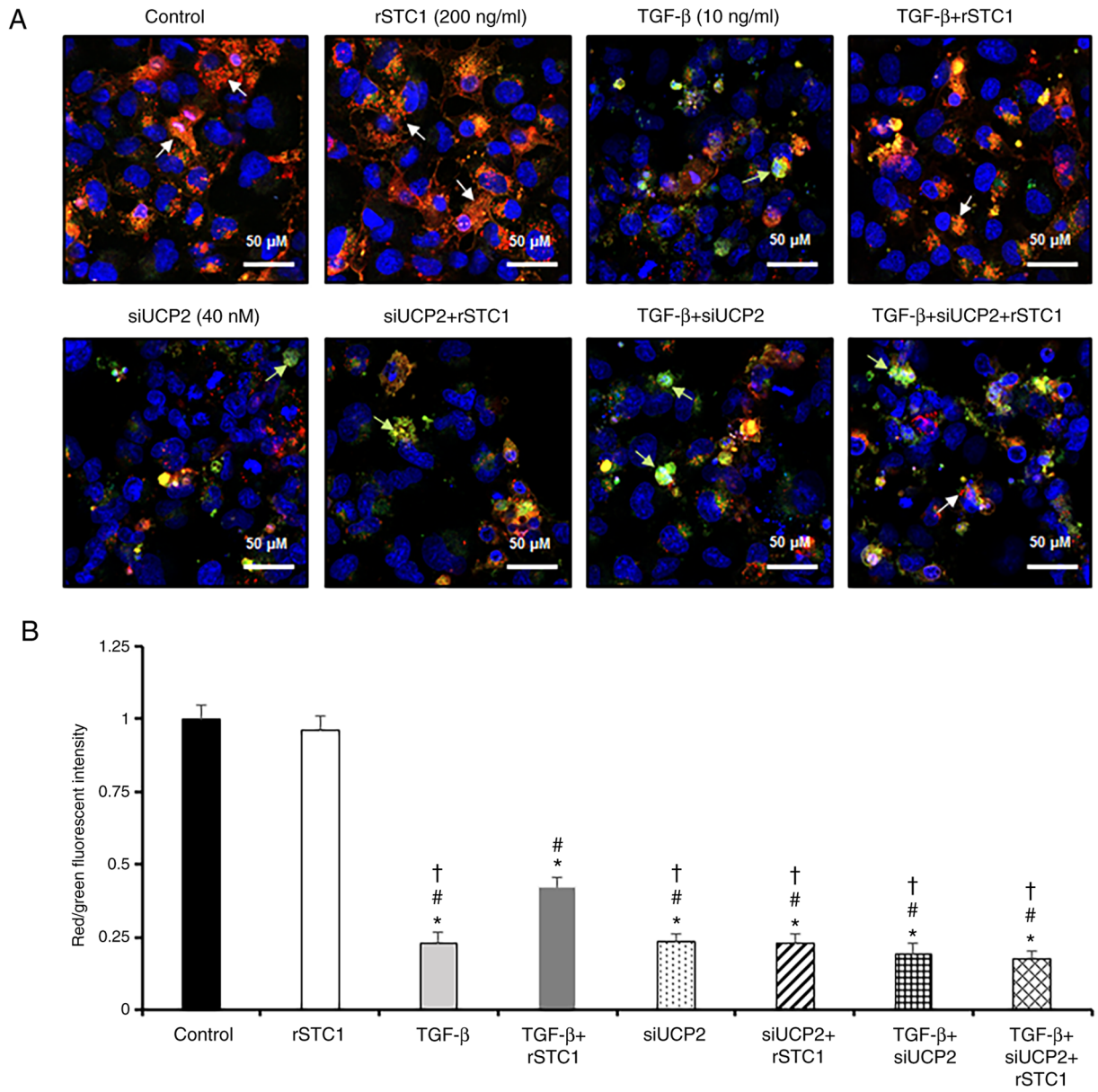

Figure 4. Effect of rSTC1 on the MMP in HK2 cells under fibrotic conditions. (A) Scanning of MMP in HK2 cells using a confocal microscope. Green fluorescence represents the monomeric form of the JC-1 molecule, which appears in the cytosol after mitochondrial membrane depolarization. Red fluorescence indicates the mitochondrial aggregate form of JC-1, indicating higher MMP). Cells were labeled with DAPI (blue) to visualize nuclei and JC-1 to visualize mitochondria. White arrow, healthy cells; green arrow, dead cells. (B) Ratio of the red to green fluorescence intensity representing the quantitative MMP in each group. *P<0.05 compared with the control; #P<0.05 compared with STC1-treated cells; †P<0.05 compared with TGF-β and STC1-treated cells. MMP, mitochondrial membrane potential; siUCP2, UCP2-targeted small interfering RNA; rSTC1, recombinant stanniocalcin-1; UCP2, uncoupling protein 2.

of siUCP2-transfected cells with rSTC1 and TGF-β together increased the expression levels of α-SMA and fibronectin compared with the levels in scrambled siRNA-transfected cells or cells treated with rSTC1 and TGF-β (Fig. 3C). These data suggest that the STC1-mediated reduction in fibrosis occurs via UCP2.

rSTC1 treatment attenuates the TGF-β-induced decrease in MMP and increase in mitochondrial ROS generation in HK2 cells. Mitochondria account for the majority of cellular ROS production, and UCP2 serves an important role in restoring MMP and dissipating metabolic energy to prevent oxidative stress (23). Since UCP2 expression was induced by rSTC1 and attenuated by TGF-β treatment, we hypothesized that STC1 might be involved in UCP2-dependent regulation of MMP and ROS generation in mitochondria. Treatment of HK2 cells with TGF-β reduced MMP levels compared with the control, as indicated by a decrease in the ratio of red/green fluorescence intensity (Fig. 4). In comparison with levels in cells treated with TGF-β alone, the present study revealed that after treatment with rSTC1 and TGF-β, the MMP level was restored, as indicated by an increase in the ratio of red/green fluorescence intensity (42% vs. 23%). To further elucidate the role of UCP2, HK2 cells pre-treated with STC1 alone or in combination with TGF-β were transfected with siUCP2. Treatment of siUCP2-transfected cells with rSTC1 and TGF-β significantly decreased the intensity of red fluorescence compared with that in cells with rSTC1 + TGF-β treatment. These data suggest

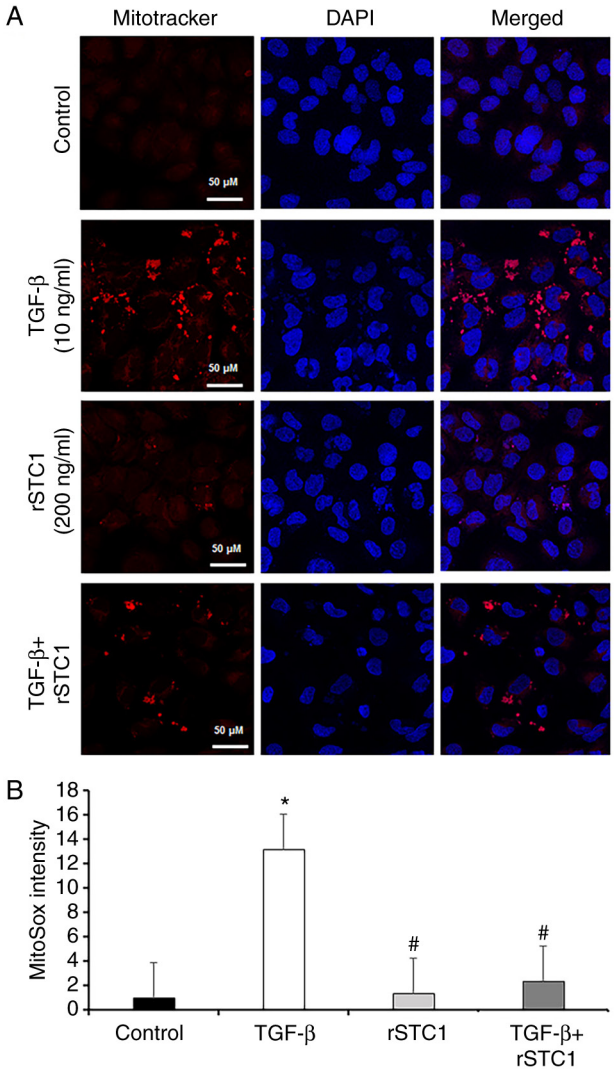

Figure 5. Mitochondrial ROS assay using MitoSOX in HK2 cells. (A) Mitochondrial ROS (magnification, x400; scale bar, 50 μm) were labeled. (B) Quantitative analysis of mitochondrial ROS production using the LMS 5 imaging software. *P<0.05 compared with the control; #P<0.05 compared with TGF-β-only-treated cells. ROS, reactive oxygen species; rSTC1, recombinant stanniocalcin-1.

that rSTC1 attenuates TGF-β-induced reductions in MMP, and this effect is dependent on UCP2. Mitochondrial UCP2 regulates oxidative stress (24) and STC1 is an effective ROS scavenger (16,17). To identify the effect of STC1 on mitochondrial ROS generation, the mitochondria-specific probe MitoSOX was used. As shown in Fig. 5B, mitochondrial ROS production was 12.9-fold higher in TGF-β-only-treated HK2 cells than in control cells. However, treatment with TGF-β and rSTC1 decreased mitochondrial ROS production to 17.5% of the levels in cells treated with TGF-β alone (Fig. 5).

Discussion

The present results suggest that STC1 protects against cellular fibrosis in kidney tubular epithelial cells based on three lines of evidence. First, TGF-β-induced fibrosis and elevated ROS production were ameliorated by rSTC1 treatment in HK2 cells. Second, the effects of rSTC1 treatment were mediated via the AMPK-UCP2 signaling pathway in HK2 cells. Third, STC1-mediated activation of the AMPK-UCP2 signaling pathway antagonized mitochondrial ROS production and the MMP decrease in HK2 cells. Therefore, the present results indicate that exogenous STC1 is a potential agent for the management of cellular fibrosis in kidney epithelial cells.

Fibrosis represents the final pathway shared by nearly all progressive CKDs (4). Although there are no targeted therapies to slow fibrosis, previous advances in CKD research have clarified the cellular and molecular mechanisms underlying the disease (5,25,26). However, few studies have evaluated the anti-fibrotic function of STC1 (27,28). Ono *et al* (27) revealed that STC1 ameliorates pulmonary fibrosis by reducing oxidative stress in a dose-dependent manner and reduces endoplasmic reticulum (ER) stress and TGF-β1 synthesis in alveolar macrophages in bleomycin-induced pulmonary fibrosis. STC1 may modulate UCP2 expression in lung cells and uncoupling respiration reduces MMP. In addition, STC1 reduce ER stress through the reduction of ROS, ameliorating pulmonary fibrosis (28). The present study revealed that STC1 upregulated AMPK and UCP2 and that an inhibitor of AMPK reduced the expression levels of UCP2 in tubular epithelial cells, suggesting that STC1 may regulate renal AMPK-UCP2 activity, as reported by Pan *et al* (19). In the present study, treatment with STC1 reduced the expression levels of fibrosis markers, such as α-SMA and fibronectin, in TGF-β-stimulated HK-2 cells.

However, the mechanism underlying the STC1-mediated inhibition of fibrosis in the kidney is unclear. We hypothesized that AMPK-UCP2 activation could rescue fibrosis by regulating MMP. AMPK is highly expressed in the kidneys, where it is considered to be involved in a variety of physiological and pathological processes (29), and a reduction in AMPK activity has been proposed as a mechanism underlying renal fibrosis in different experimental models of CKD (30-33). Mechanisms underlying the inhibition of fibrosis by AMPK activation have been reported (31,32). TGF-β1, which serves a prominent role in fibrosis, diminishes AMPK phosphorylation and increases fibrosis (22,31). By contrast, the pharmacologic activation of AMPK reverses the fibrogenic response induced by TGF-β (32). Similar to the results of a previous study by Pan *et al* (19), the present study revealed that AMPK inhibition restored the STC1-mediated attenuation of TGF-β-induced upregulation of α-SMA and fibronectin in HK2 cells. This result suggested that the anti-fibrotic effect of STC1 is mediated by AMPK activity.

AMPK increases the expression of several antioxidant genes, such as superoxide dismutase (16), UCP2 and nuclear factor erythroid-2-related factor (34). Among them, UCP2 regulates the production of mitochondrial ROS (27,28). The optimal production of mitochondrial ROS is essential for mitochondrial biogenesis; however, increased ROS production exceeding local antioxidant capacities is associated with mitochondrial dysfunction, mitochondrial DNA damage and aberrant metabolism (35,36). Mitochondrial damage triggers cell signaling pathways that can cause ROS overproduction, resulting in oxidative stress, which serves crucial roles in the pathogenesis of renal fibrosis (37,38). The role of UCP2 in renal disease has been explored in the context of acute kidney injury and diabetic nephropathy (24,39). UCP2 ameliorates

mitochondrial dysfunction and oxidative stress in lipopolysaccharide-induced acute kidney injury (39) and UCP2 deletion aggravates tubular injury in ischemia-reperfusion injury by inducing ROS overproduction (40), which highlights the importance of these transporters in ROS dissipation. Additionally, under disease conditions, the deletion of UPC2 may contribute to the ameliorate of kidney fibrosis by inhibiting macrophage infiltration (41,42). The present results revealed that the upregulation of UCP2 by STC1 reduced fibrosis markers induced by TGF-β in HK2 cells and UCP2 silencing in cells treated with rSTC1 and TGF-β increased the levels of fibrosis markers, such as α-SMA and fibronectin. The effect of STC1 in cellular fibrosis was diminished by UCP2 suppression. Therefore, we hypothesize that the inhibitory effect of STC1 on cellular fibrosis is mediated via the AMPK-UCP2 signaling pathway.

Mitochondrial STC1 suppresses ROS generation through the induction of UCP expression (16,18) and serves an important role in the regulation of mitochondrial function (43). Increased UCP2 expression in the tubular epithelium of STC1 transgenic animal kidneys is associated with lower superoxide generation (18). Excessive production of mitochondrial ROS is linked to mitochondrial dysfunction, which causes cellular damage and the progression of renal disease (5,6). TGF-β, a key driver of renal fibrosis, induces oxidative stress and mitochondrial dysfunction (6), as evidenced by the marked decrease in MMP and increase in mitochondrial ROS production in HK2 cells (44). Mitochondrial dysfunction-induced renal fibrosis has attracted immense research attention since the early 2000s (5). The kidneys have high energy requirements, and thus, kidney cells contain several mitochondria. Mitochondrial dysfunction serves a crucial role in the pathogenesis of CKD, and studies have demonstrated that mitochondrial dysfunction is involved in the pathological development of renal fibrosis (5,11,45). Mitochondrial dysfunction promotes inflammation and fibrotic responses, which induces tubulointerstitial fibrosis and various forms of CKD, including diabetic and IgA nephropathy (6,35). In the present study, TGF-β-mediated fibrosis involved the enhanced generation of mitochondrial ROS and loss of MMP via the AMPK-UCP2 signaling pathway. The observed changes in MMP may lead to mitochondrial dysfunction and occur as a consequence of ROS generation by TGF-β (46). The total force driving protons into the mitochondria is a combination of the MMP and mitochondrial pH gradient (47). The proton electrochemical gradient potential provides the charge gradient required for mitochondrial Ca^{2+} sequestration and regulates ROS production; thus, it is also a central regulator of cellular health (47). TGF-β-induced MMP loss was reduced by STC1, and this effect was diminished by knocking down UCP2 expression using siUCP2.

The present study demonstrated a protective role of exogenous STC1 in TGF-β-induced cellular fibrosis in HK2 cells. STC1 treatment attenuated TGF-β-induced fibrosis by reducing mitochondrial ROS production via the AMPK-UCP2 pathway. To establish the role of STC1 in renal fibrosis, further research using animals may be required to confirm the results of the present study.

Acknowledgements

Not applicable.

Funding

This work was supported by the Individual Basic Science and Engineering Research Program of the Ministry of Education of the Republic of Korea and National Research Foundation of Korea (grant no. NRF-2016R1D1A1B03933207), the National Research Foundation of Korea (NRF) funded by the Korean government (MSIT) (grant nos. NRF-2019R1A2C2086276 and NRF-2020R1A2C1003310), and the grant of Chonnam National University Hospital Biomedical Research Institute (grant no. BCRI-22079).

Availability of data and materials

The datasets used and/or analyzed during the current study are available from the corresponding author on reasonable request.

Authors' contributions

SWK conceived and designed the experiments. EMY, JSP and SYJ performed the experiments. EHB and JSP analyzed the data and confirm the authenticity of all the raw data. SKM contributed to interpretation of data. EMY wrote the paper. SWK and SKM contributed to critical revisions of the paper. All authors read and approved the final manuscript.

Ethics approval and consent to participate

Not applicable.

Patient consent for publication

Not applicable.

Competing interests

The authors declare that they have no competing interests.

References

1. Jha V, Garcia-Garcia G, Iseki K, Li Z, Naicker S, Plattner B, Saran R, Wang AYM and Yang CW: Chronic kidney disease: Global dimension and perspectives. Lancet 382: 260-272, 2013.
2. Vallianou NG, Mitesh S, Gkogkou A and Geladari E: Chronic kidney disease and cardiovascular disease: Is there any relationship? Curr Cardiol Rev 15: 55-63, 2019.
3. Bello AK, Alrukhaimi M, Ashuntantang GE, Basnet S, Rotter RC, Douthat WG, Kazancioglu R, Köttgen A, Nangaku M, Powe NR, *et al*: Complications of chronic kidney disease: Current state, knowledge gaps, and strategy for action. Kidney Int Suppl (2011) 7: 122-129, 2011.
4. He J, Xu Y, Koya D and Kanasaki K: Role of the endothelial-to-mesenchymal transition in renal fibrosis of chronic kidney disease. Clin Exp Nephrol 17: 488-497, 2013
5. Quadri MM, Fatima SS, Che RC and Zhang AH: Mitochondria and renal fibrosis. Adv Exp Med Biol 1165: 501-524, 2019.
6. Bhargava P and Schnellmann RG: Mitochondrial energetics in the kidney. Nat Rev Nephrol 13: 629-646, 2017.
7. Ishimoto Y and Inagi R: Mitochondria: A therapeutic target in acute kidney injury. Nephrol Dial Transplant 31: 1062-1069, 2016.
8. Kaushal GP, Chandrashekar K and Juncos LA: Molecular interactions between reactive oxygen species and autophagy in kidney disease. Int J Mol Sci 20: 3791, 2019.
9. Coughlan MT and Sharma K: Challenging the dogma of mitochondrial reactive oxygen species overproduction in diabetic kidney disease. Kidney Int 90: 272-279, 2016.

10. Tsuji N, Tsuji T, Ohashi N, Kato A, Fujigaki Y and Yasuda H: Role of mitochondrial DNA in septic AKI via toll-like receptor 9. J Am Soc Nephrol 27: 2009-2020, 2016.
11. Che R, Yuan Y, Huang S and Zhang A: Mitochondrial dysfunction in the pathophysiology of renal diseases. Am J Physiol Renal Physiol 306: 367-378, 2014.
12. Yeung BH, Law AY and Wong CK: Evolution and roles of stanniocalcin. Mol Cell Endocrinol 349: 272-280, 2012.
13. Ishibashi K and Imai M: Prospect of a stanniocalcin endocrine/paracrine system in mammals. Am J Physiol Renal Physiol 282: F367-F375, 2002.
14. McCudden CR, James KA, Hasilo C and Wagner GF: Characterization of mammalian stanniocalcin receptors. Mitochondrial targeting of ligand and receptor for regulation of cellular metabolism. J Biol Chem 277: 45249-4558, 2002.
15. Ellard JP, McCudden CR, Tanega C, James KA, Ratkovic S, Staples JF and Wagner GF: The respiratory effects of stanniocalcin-1 (STC-1) on intact mitochondria and cells: STC-1 uncouples oxidative phosphorylation and its actions are modulated by nucleotide triphosphates. Mol Cell Endocrinol 264: 90-101, 2007.
16. Wang Y, Huang L, Abdelrahim M, Cai Q, Truong A, Bick R, Poindexter B and Sheikh-Hamad D: Stanniocalcin-1 suppresses superoxide generation in macrophages through induction of mitochondrial UCP2. J Leukoc Biol 86: 981-988, 2009.
17. Sheikh-Hamad D: Mammalian stanniocalcin-1 activates mitochondrial antioxidant pathways: New paradigms for regulation of macrophages and endothelium. Am J Physiol Renal Physiol 298: F248-F254, 2010.
18. Huang L, Belousova T, Chen M, DiMattia G, Liu D and Sheikh-Hamad D: Overexpression of stanniocalcin-1 inhibits reactive oxygen species and renal ischemia/reperfusion injury in mice. Kidney Int 82: 867-877, 2012.
19. Pan JS, Huang L, Belousova T, Lu L, Yang Y, Reddel R, Chang A, Ju H, DiMattia G, Tong Q, *et al*: Stanniocalcin-1 inhibits renal ischemia/reperfusion injury via an AMP-activated protein kinase-dependent pathway. J Am Soc Nephrol 26: 364-378, 2015.
20. Meng XM, Nikolic-Paterson DJ and Lan HY: TGF-β: The master regulator of fibrosis. Nat Rev Nephrol 12: 325-338, 2016.
21. Sivandzade F, Bhalerao A and Cucullo L: Analysis of the mitochondrial membrane potential using the cationic JC-1 dye as a sensitive fluorescent probe. Bio Protoc 9: e3128, 2019.
22. Kim H, Moon SY, Kim JS, Baek CH, Kim M, Min JY and Lee SK: Activation of AMP-activated protein kinase inhibits ER stress and renal fibrosis. Am J Physiol Renal Physiol 308: F226-F236, 2015.
23. Andreyev AY, Kushnareva YE and Starkov AA: Mitochondrial metabolism of reactive oxygen species. Biochemistry (Mosc) 70: 200-214, 2005.
24. Donadelli M, Dando I, Fiorini C and Palmieri M: UCP2, a mitochondrial protein regulated at multiple levels. Cell Mol Life Sci 71: 1171-1190, 2014.
25. Humphreys BD: Mechanisms of renal fibrosis. Annu Rev Physiol 80: 309-326, 2018.
26. Djudjaj S and Boor P: Cellular and molecular mechanisms of kidney fibrosis. Mol Aspects Med 65: 16-36, 2019.
27. Ono M, Ohkouchi S, Kanehira M, Tode N, Kobayashi M, Ebina M, Nukiwa T, Irokawa T, Ogawa H, Akaike T, *et al*: Mesenchymal stem cells correct inappropriate epithelial-mesenchyme relation in pulmonary fibrosis using stanniocalcin-1. Mol Ther 23: 549-560, 2015.
28. Ohkouchi S, Ono M, Kobayashi M, Hirano T, Tojo Y, Hisata S, Ichinose M, Irokawa T, Ogawa H and Kurosawa H: Myriad functions of stanniocalcin-1 (STC1) cover multiple therapeutic targets in the complicated pathogenesis of idiopathic pulmonary fibrosis (IPF). Clin Med Insights Circ Respir Pul Med 9: 91-96, 2015.
29. Juszczak F, Caron N, Mathew AV and Declèves AE: Critical role for AMPK in metabolic disease-induced chronic kidney disease. Int J Mol Sci 21: 7994, 2020.
30. Sharma K: Obesity, oxidative stress, and fibrosis in chronic kidney disease. Kidney Int Suppl (2011) 4: 113-117, 2017.
31. Thakur S, Viswanadhapalli S, Kopp JB, Shi Q, Barnes JL, Block K, Gorin Y and Abboud HE: Activation of AMP-activated protein kinase prevents TGF-β1-induced epithelial-mesenchymal transition and myofibroblast activation. Am J Pathol 185: 2168-2180, 2015.
32. Gao J, Ye J, Ying Y, Lin H and Luo Z: Negative regulation of TGF-β by AMPK and implications in the treatment of associated disorders. Acta Biochim Biophys Sin (Shanghai) 50: 523-531, 2018.
33. Borges CM, Fujihara CK, Malheiros D, de Ávila VF, Formigari GP and Lopes de Faria JB: Metformin arrests the progression of established kidney disease in the subtotal nephrectomy model of chronic kidney disease. Am J Physiol Renal Physiol 318: F1229-F1236, 2020.
34. Trewin AJ, Berry BJ and Wojtovich AP: Exercise and mitochondrial dynamics: Keeping in shape with ROS and AMPK. Antioxidants (Basel) 7: 7, 2018.
35. Bhatia D, Capili A and Choi ME: Mitochondrial dysfunction in kidney injury, inflammation, and disease: Potential therapeutic approaches. Kidney Res Clin Pract 39: 244-258, 2020.
36. Czajka A, Ajaz S, Gnudi L, Parsade CK, Jones P, Reid F and Malik AN: Altered mitochondrial function, mitochondrial DNA and reduced metabolic flexibility in patients with diabetic nephropathy. EBioMedicine 2: 499-512, 2015.
37. Su H, Wan C, Song A, Qiu Y, Xiong W and Zhang C: Oxidative stress and renal fibrosis: Mechanisms and therapies. Adv Exp Med Biol 1165: 585-604, 2019.
38. Lv W, Booz GW, Fan F, Wang Y and Roman RJ: Oxidative stress and renal fibrosis: Recent isights for the development of novel therapeutic strategies. Front Physiol 9: 105, 2018.
39. Ding Y, Zheng Y, Huang J, Peng W, Chen X, Kang X and Zeng Q: UCP2 ameliorates mitochondrial dysfunction, inflammation, and oxidative stress in lipopolysaccharide-induced acute kidney injury. Int Immunopharmacol 71: 336-349, 2019.
40. Zhou Y, Cai T, Xu J, Jiang L, Wu J, Sun Q, Zen K and Yang J: UCP2 attenuates apoptosis of tubular epithelial cells in renal ischemia-reperfusion injury. Am J Physiol Renal Physiol 313: F926-F937, 2017.
41. Wynn TA and Vannella KM: Macrophages in tissue repair, regeneration, and fibrosis. Immunity 44: 450-462, 2016.
42. Anders HJ and Ryu M: Renal microenvironments and macrophage phenotypes determine progression or resolution of renal inflammation and fibrosis. Kidney Int 80: 915-925, 2011.
43. Zhang Y, Shan P, Srivastava A, Li Z and Lee PJ: Endothelial stanniocalcin 1 maintains mitochondrial bioenergetics and prevents oxidant-induced lung injury via toll-like receptor 4. Antioxid Redox Signal 30: 1775-1796, 2019.
44. Abe Y, Sakairi T, Beeson C and Kopp JB: TGF-β1 stimulates mitochondrial oxidative phosphorylation and generation of reactive oxygen species in cultured mouse podocytes, mediated in part by the mTOR pathway. Am J Physiol Renal Physiol 305: F1477-F1490, 2013.
45. Galvan DL, Green NH and Danesh FR: The hallmarks of mitochondrial dysfunction in chronic kidney disease. Kidney Int 92: 1051-1057, 2017.
46. Ribeiro A, Bronk SF, Roberts PJ, Urrutia R and Gores GJ: The transforming growth factor beta(1)-inducible transcription factor TIEG1, mediates apoptosis through oxidative stress. Hepatology 30: 1490-1497, 1999.
47. Perry SW, Norman JP, Barbieri J, Brown EB and Gelbard HA: Mitochondrial membrane potential probes and the proton gradient: A practical usage guide. Biotechnique 50: 98-115, 2011.